Electronic Supplementary Information for

Transition metal complex-incorporated polyaniline as a platform for enzymatic uric acid electrochemical sensor

Ruth Stephanie,[‡] Dae Yeon Lee,[‡] Chan Yeong Park[*], and Tae Jung Park[*]

Department of Chemistry, Research Institute of Chem-Bio Diagnostic Technology, Chung-Ang University, 84 Heukseok-ro, Dongjak-gu, Seoul 06974, Republic of Korea

*Corresponding author. Tel.: +82-2-820-5220; fax: +82-2-825-4736.

E-mail address: pcyzzing@naver.com (C.Y. Park); tjpark@cau.ac.kr (T.J. Park)

[‡]These authors equally contributed to this work.

Electrochemical surface area comparison between PANI-RC and PANI-RC/EM/GA

The active surface area of the samples is determined using Randles-Sevcik equation according to Equation S1. The CV was carried out with 5 mM $[Fe(CN)_6]^{3-/4-}$ in 0.1 M KCl at the scan rate of 50 mV/s.

$$I_p = 2.69 \times 10^5 \times A \times C \times D^{1/2} \times n^{3/2} \times v^{1/2} \qquad \text{(Equation S1)}$$

with:
I_p = Current peak from CV (A)

A = Surface area (cm^2)

C = Concentration of analyte (mol/cm^3)

D = Diffusion coefficient (cm^2/s)

n = number of electrons participating in the reaction (In our case, n = 1)
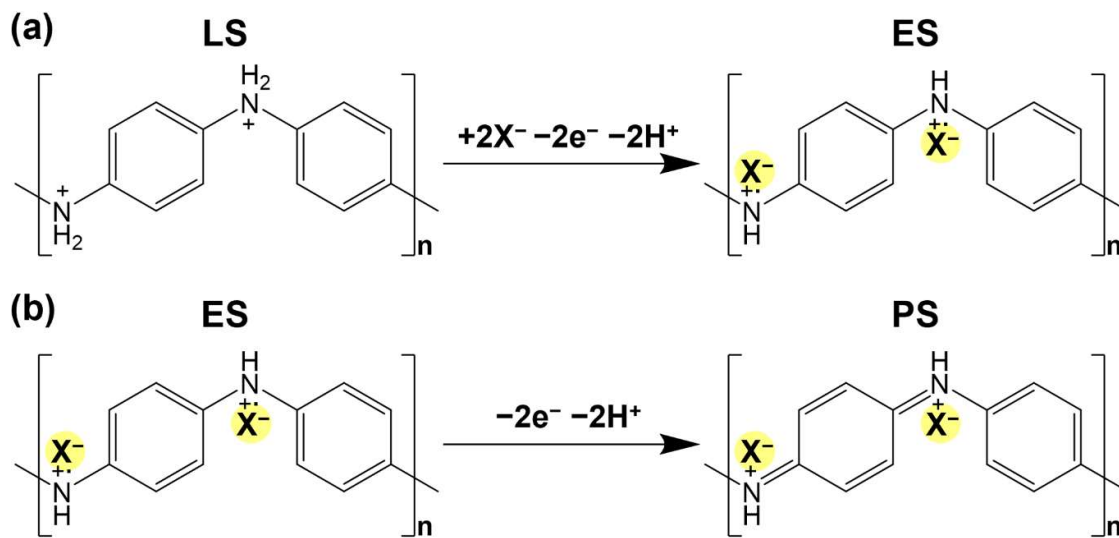
v = Scan rate (V/s)

Figure S1. Mechanism of PANI (and PANI-RC) polymerization, involving three oxidation states. Transition from (a) LS to ES and (b) ES to PS. The highlighted yellow part is where $[Fe(CN)_6]^{3-/4-}$ are positioned on the backbone of PANI ([*]Note: LS: leucoemeraldine salt, ES: emeraldine salt, PS: pernigraniline salt).
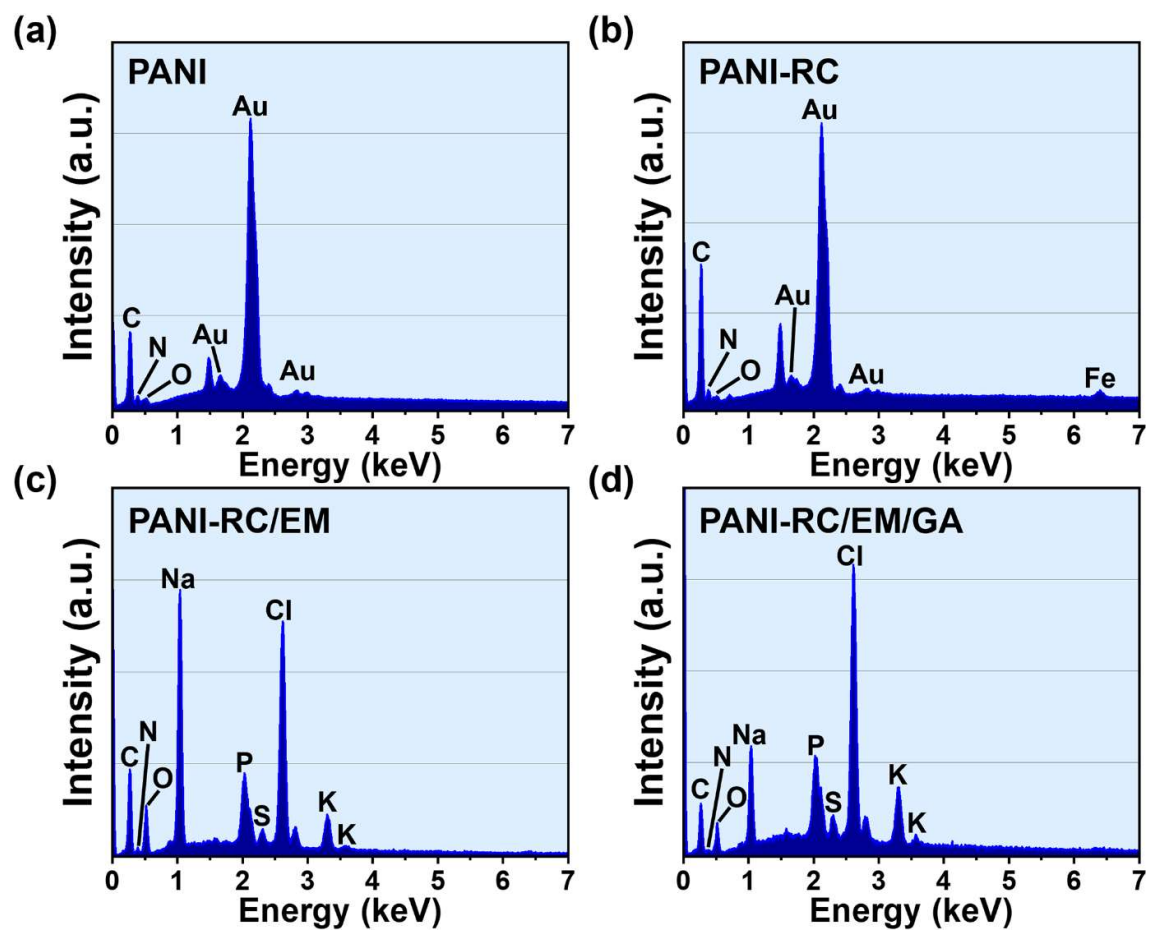
Figure S2. EDS spectra of (a) PANI, (b) PANI-RC, (c) PANI-RC/EM, and (d) PANI-RC/EM/GA.
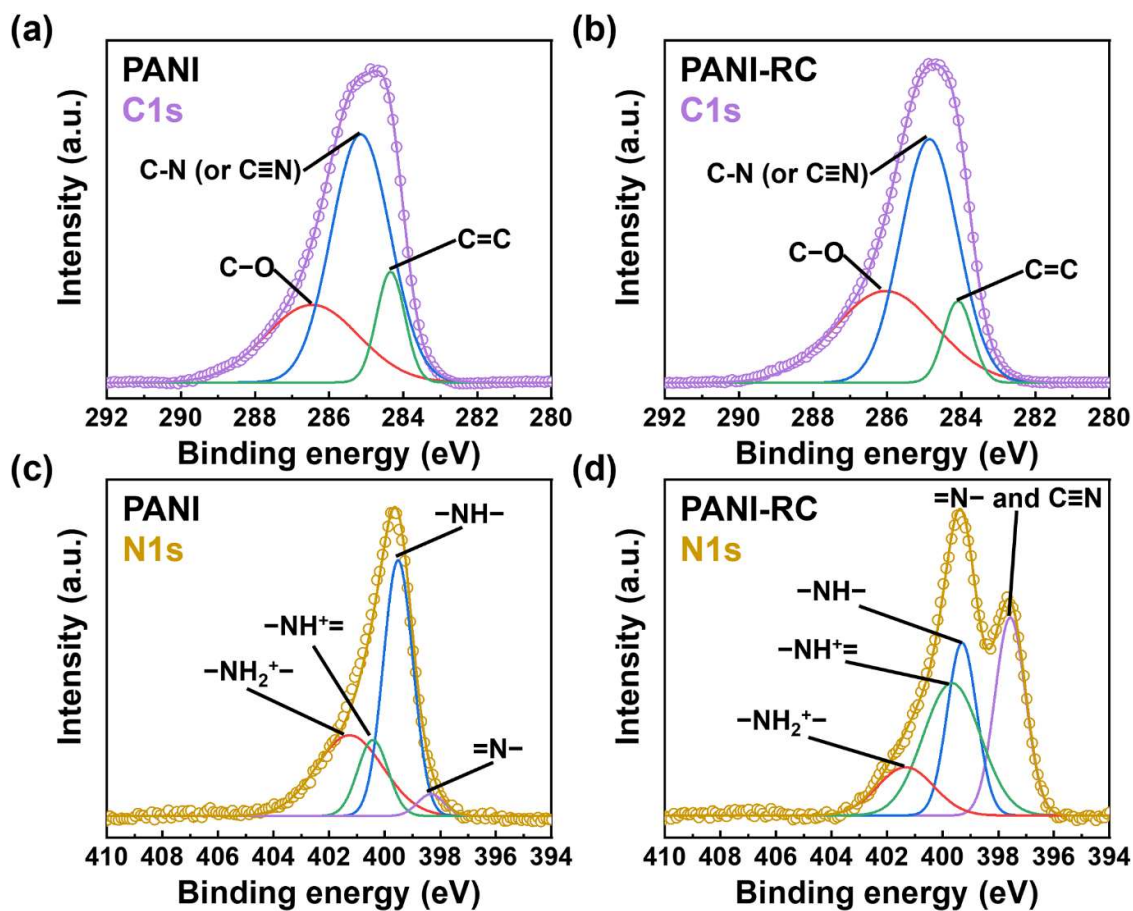
Figure S3. Narrow range XPS spectra of PANI and PANI-RC. C1s region of (a) PANI and (b) PANI-RC. N1s region of (c) PANI and (d) PANI-RC.
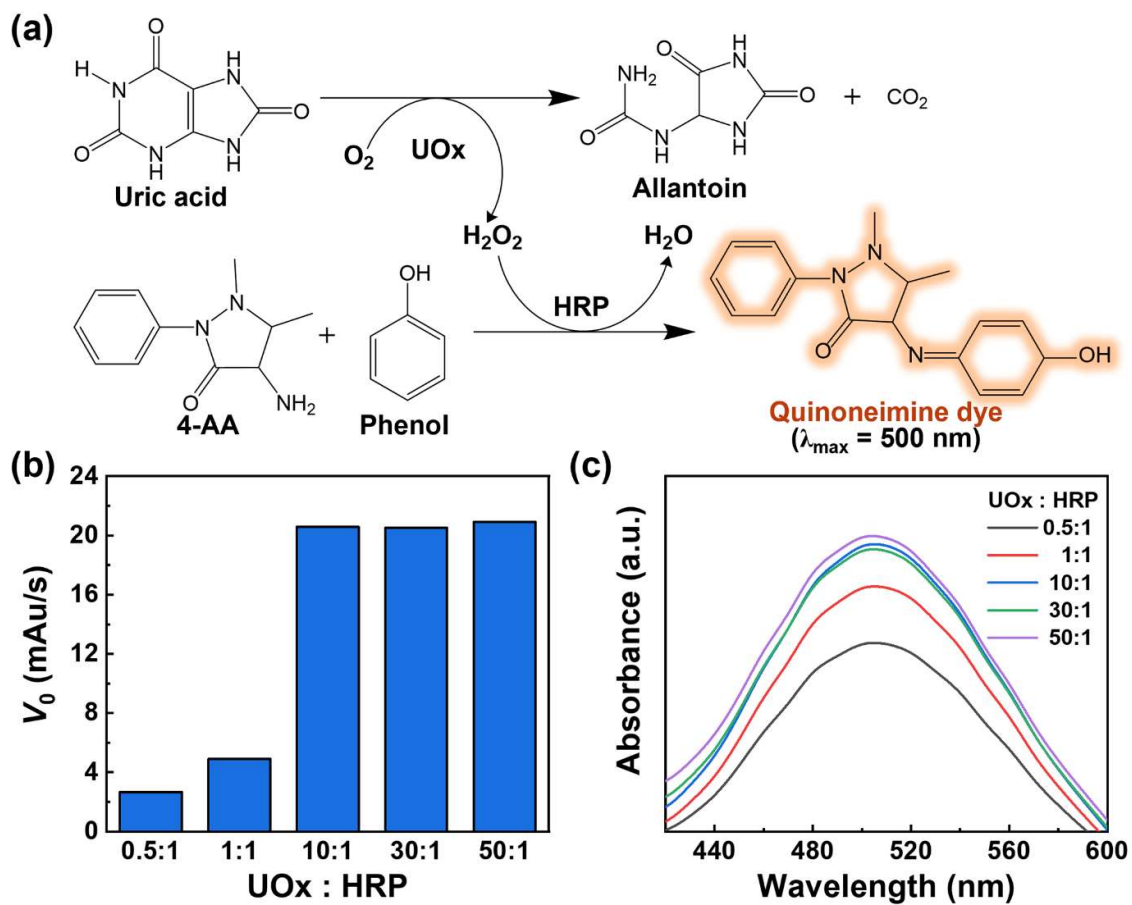
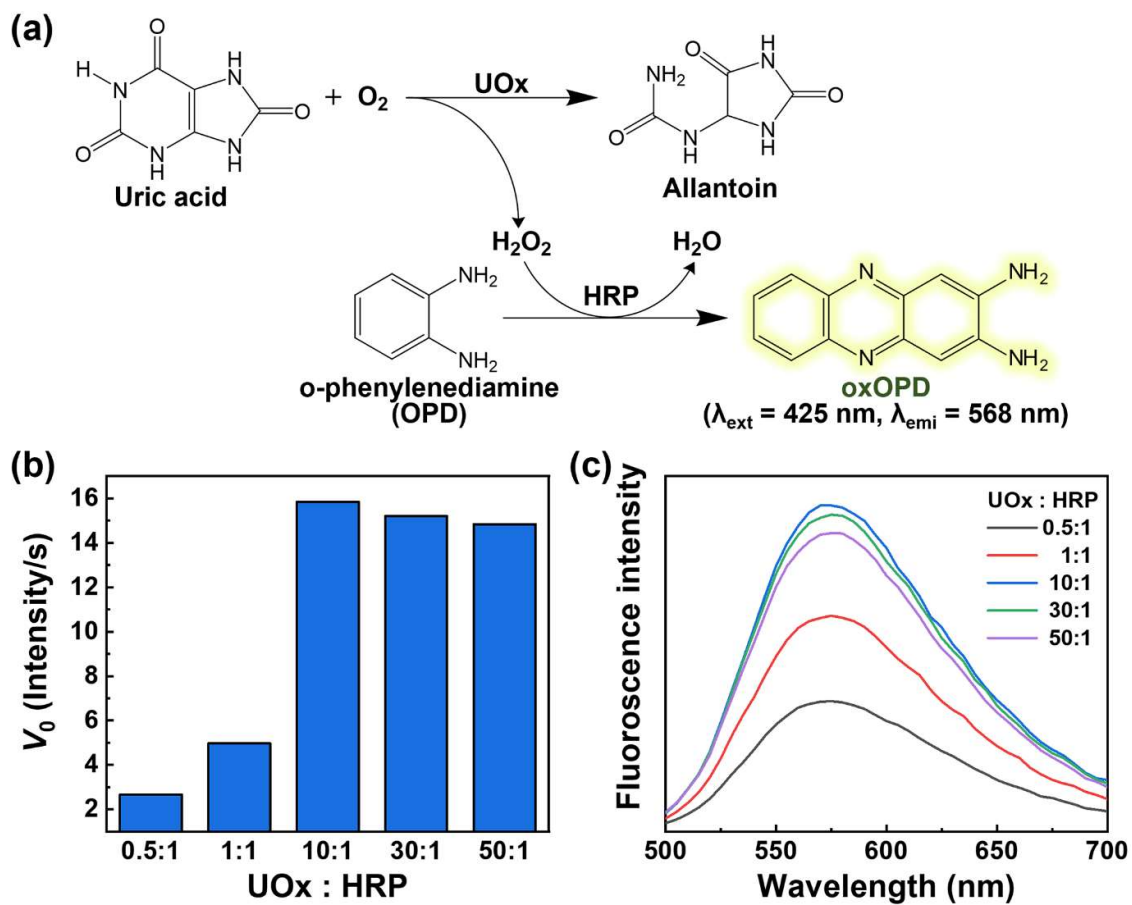**Figure S4.** (a) Mechanism of 4-AA method. (b) UOx : HRP ratio optimization. (c) Absorbance spectra.

Figure S5. (a) Mechanism of OPD method. (b) UOx : HRP ratio optimization. (c) Fluorescence spectra.

(a)

(b)

(c)

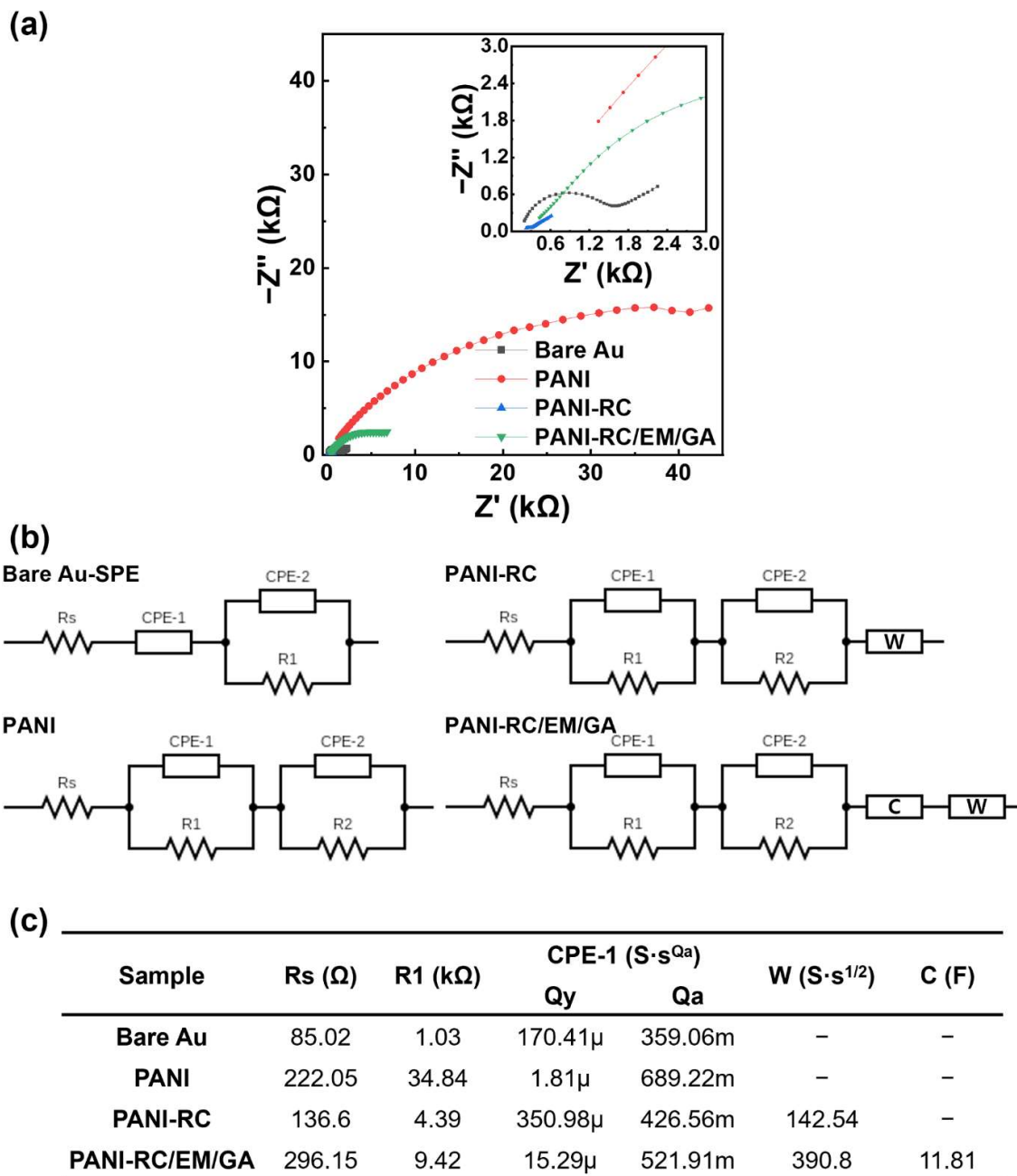| Sample	Rs (Ω)	R1 (kΩ)	CPE-1 (S·s^Qa)		W (S·s^{1/2})	C (F)
			Qy	Qa		
Bare Au	85.02	1.03	170.41μ	359.06m	–	–
PANI	222.05	34.84	1.81μ	689.22m	–	–
PANI-RC	136.6	4.39	350.98μ	426.56m	142.54	–
PANI-RC/EM/GA	296.15	9.42	15.29μ	521.91m	390.8	11.81

Figure S6. (a) Nyquist plot of each synthesis step in the making of PANI-RC/EM/GA, and (b) the respective equivalent circuits. (c) The change of impedance elements recorded from the EIS of each synthesis step in the making of PANI-RC/EM/GA.

Table S1. FT-IR peak assignments observed in FT-IR spectrum

Material	Assignments	Chemical bonding	Wavenumber (cm^{-1})
PANI	Quinonoid (Q) ring stretching	N=Q=N	1563
	Benzenoid (B) ring stretching	N−B−N	1484
	C−N stretching of secondary aromatic amine	C−N	1295
	C−N$^{\cdot+}$ in the polaron lattice of PANI	C−N$^{\cdot+}$	1241
	Q=NH$^+$−B or B−NH$^{\cdot+}$−B	C−H	1140
	(1,4-disubstituted ring)/Q ring deformation	C−H	818
PANI-RC	C≡N stretching vibrational peak	C≡N	2045
	N–H stretching vibration of secondary amine	N−H	3417
PANI-RC/EM	O−H stretching vibrations	−OH	3067
	C−H stretching of alkane	−CH, −CH$_2$, −CH$_3$	2963, 2872
	C=O stretching vibrations of amide I	C=O	1652
	−CH$_2$ scissoring vibrations	−CH$_2$	1401
PANI-RC/EM/GA	C−O stretching vibrations of aldehydes	C−O	1711

Table S2. Raman peak assignments comparison between PANI and PANI-RC

Structure	Raman shift peak (cm^{-1})	
	PANI	PANI-RC
Aromatic ring	417, 518	424, 522
C-H bending vibrations of the semiquinone rings	1171	1171
C-N benzenoid	1171	1171
Localized and delocalized polarons (C-N^{+} polaronic form)	1340, 1377	1340, 1374
C=N quinoid (N-H deformation vibration associated with the semiquinone structure)	1505	1505
C=C quinoid (C=C stretches vibration in quinoid ring)	1587	1600